

Combing of Molecules in Microchannels (COMMIC): A Method for Micropatterning and Orienting Stretched Molecules of DNA on a Surface

Cécilia A. P. Petit and Jeffrey D. Carbeck*

Department of Chemical Engineering, Princeton University, Engineering Quadrangle, Olden Street, Room A319, Princeton, New Jersey 08544

Received May 25, 2003; Revised Manuscript Received June 14, 2003

ABSTRACT

This paper presents a new method for creating microscopic patterns of stretched and oriented molecules of DNA on a surface. Combing of molecules in microchannels (COMMIC), a process by which molecules are deposited and stretched onto a surface by the passage of an air–water interface, creates these patterns. This approach demonstrates that the direction of stretching of the molecules is always perpendicular to the air–water interface; the shape and motion of this interface serve as an effective local field directing the chains dynamically as they are stretched onto the surface. The geometry of the microchannel directs the placement of the DNA molecules, while the geometry of the air–water interface directs the local orientation and curvature of the molecules. This ability to control both the placement and orientation of chains has implication for the use of COMMIC in genetic analysis and in the bottom-up approach to nanofabrication.

Introduction. The “bottom-up” approach to the fabrication of nanoscale systems starts with the controlled deposition of molecules or nanoscale objects (such as rods, wires, or tubes) on a surface;¹ these objects serve as templates that direct the deposition of additional molecules or materials. This approach to nanofabrication places the following requirements on the templates. First, the placement of the templates must be controlled on microscopic and nanoscopic length scales. Second, the templates must be able to adopt different, well-defined shapes and orientations. Finally, the templates must be programmable objects such that they present specific sites for the further attachment of functional building blocks and allow integration into devices and systems.² In this paper, we support the proposition that DNA molecules are ideal templates for bottom-up nanofabrication.^{3–7}

Previous work has demonstrated that DNA satisfies the last of these requirements as a template. For example, Keren et al. showed that sequence-specific molecular lithography is possible; they used proteins that bind to specific sites on DNA to create patterns of metal coatings on single molecules of DNA.⁸ The objective of this work is to demonstrate that DNA also satisfies the other two requirements for a template. We do so by stretching and orienting individual DNA molecules in microscopic channels. The geometry of the channels directs the placement of molecules, while the

geometry of the air–water interface, which stretches the DNA within the channels, directs the shape and orientation of the molecules. We refer to this technique as the combing of molecules in microchannels, or COMMIC.

Molecular combing, a method by which molecules of DNA are deposited and stretched onto a surface, was originally developed as a technique for genetic analysis on whole chromosomes.^{9,10} The mechanism proposed by Ben-simon et al. states that under specific values of the pH and ionic strength, the partial melting of the ends of the DNA molecules exposes their hydrophobic core, which adsorbs onto a hydrophobic surface.¹¹ As the solution is removed from the surface, the air–water interface moves past the end-adsorbed molecules, stretching them as they are deposited onto the surface.

The first reported technique for combing molecules of DNA involved the recession of the meniscus as a solution containing DNA dried between two sheets of glass.⁹ Because this evaporation technique led to DNA molecules that were stretched in a sunburst pattern, it was proposed that the force responsible for stretching the molecules was exerted on the DNA locally at the air–water interface. This effect was described using a simple continuum wetting model in which the force acting on each molecule is the product of the surface tension of the air–liquid interface and the length over which this tension is exerted (i.e., the line of contact between the air–water interface and the DNA molecule). This model is

* Corresponding author. Phone: (609) 258-1331. Fax: (609) 258-0211. E-mail: jcarbeck@princeton.edu.

expressed in eq 1, where the force (F , N) is proportional to the surface tension of the air–water interface (γ_{LV} , N/m) and the diameter (d , m) of a single DNA molecule.

$$F = \gamma\pi d \quad (1)$$

In effect, the force that stretches the chain is the result of the work required to pull the chain through the air–water interface. This model assumes that the chain is wet completely by the water (i.e., it has a contact angle of zero) and predicts that stretching will occur in a direction perpendicular to the air–water interface.⁹

Using this simple model as a guide, the same group refined the combing process to deposit molecules over large surfaces with parallel alignment of the chains. They did so by pulling the surface out of the solution containing DNA that had been allowed to end-attach to the surface.¹² DNA immobilized by molecular combing retains some of its biological activity, such as the ability to bind proteins and to hybridize with complementary single-stranded DNA. These properties allowed the application of molecular combing to genetic diagnostics, such as quantifying the length of microdeletions¹² and the copy number in replicated oncogenes.¹³ The technique of molecular combing has also been used to study the activity of DNA polymerase¹⁴ and to provide a template for the fabrication of palladium nanowires.¹⁵

While several methods exist for extending DNA molecules on a surface,^{16–20} we limit our discussion to the growing number of variants of molecular combing. This focus reflects the unique ability of molecular combing to direct the instantaneous orientation of molecules during the stretching process, as discussed in this paper. Other macroscopic techniques for combing molecules include the dragging of a droplet of solution over the surface using the edge of a coverslip²¹ or a glass capillary.²²

If molecular combing is to be useful as a tool for nanofabrication and genetic analyses, the technique must be modified to produce micropatterned arrays of DNA with control over both the placement and the orientation of the molecules. Attempts to produce arrays of stretched molecules of DNA have been reported. In one example, DNA molecules were deposited onto a surface by spotting droplets of DNA solution into square arrays, followed by air-drying; the DNA was stretched as the droplets dried, producing circles approximately 500 μm in diameter.²³ In a second example, a microcapillary was used to move a drop of solution containing DNA on a surface and thereby direct the deposition of stretched DNA molecules in predetermined areas a few hundred microns in size.²² In both cases, the inherent curvature of the droplet caused the DNA to stretch in multiple directions, which would complicate the automated addressing and analysis of these arrays.

In this paper, we demonstrate the patterning of stretched molecules of DNA on the microscale by using the flow of fluid in microfabricated channels to comb double-stranded chains of DNA. We show the advantages of this method in terms of controlling both the location and the orientation of

the deposited DNA molecules. We demonstrate control over the shape of the air–water interface receding inside the microchannels by manipulating the dimensions of the channel, its wall chemistry, and the rate of fluid withdrawal. We show that the air–water interface dictates the instantaneous orientation of the molecules as they are stretched. We further take advantage of this local effect of the air–water interface to produce stretched and oriented single molecules of DNA with well-defined shapes, from straight lines, to curved molecules with tunable radii of curvature. In this way, the shape and motion of the air–water interface serve as an effective local field directing the orientation of the DNA dynamically as it is stretched onto the surface.

Results and Discussion. To investigate the effects of combing in microchannels on the placement and orientation of stretched molecules of DNA, we varied the width of the channels and the rate of withdrawal of the air–water interface. In all cases reported, the channel depth is kept constant at 40 μm .^{24,25}

The Shape of the Air–Water Interface Directs the Orientation of the Stretched DNA. We first consider the case of combing molecules of λ -phage DNA in a 100 μm wide channel fabricated from poly(dimethylsiloxane) (PDMS) and used as synthesized. In this case the PDMS is hydrophobic and displays a static contact angle of 100°, as measured by the sessile drop method. If no external pressure is applied after filling the channel with a solution containing DNA, the air–liquid interface recedes spontaneously with a convex shape, as shown in Figure 1A. When stretched under these conditions, DNA molecules were oriented in a half-sunburst pattern, as shown in Figure 1B, which is a fluorescence micrograph of DNA dyed with YOYO-1; the shape of the interface is superimposed. DNA molecules longer than 10 kilobases are often sheared as the solution is pipetted, which is responsible, in part, for the variations observed in the lengths of stretched DNA. In addition, molecules sometimes attach at both extremities, which leads to a shorter apparent stretched length.

The composite images in Figure 1 clearly show that the DNA is stretched perpendicular to the air–water interface, which is consistent with the simple wetting model described by eq 1. If the DNA were elongated by shear forces, all molecules would be aligned in the direction of the flow: that is, parallel to the walls. Although the model described by eq 1 may be too simplistic to accurately describe the molecular scale forces that stretch and orient molecules of DNA, it does appear to be useful for predicting how the shape of the air–water interface affects the orientation of the molecules of DNA.

The spontaneous recession of the DNA solution in the absence of external forces, which produced the convex air–water interface shown in Figure 1A, is likely due to capillary action. While one typically considers the filling of a hydrophilic glass capillary with water, our system exhibits the spontaneous displacement of water in a hydrophobic channel by air. The wetting of a static drop of liquid on a solid surface is described by Young's equation,²⁶ which

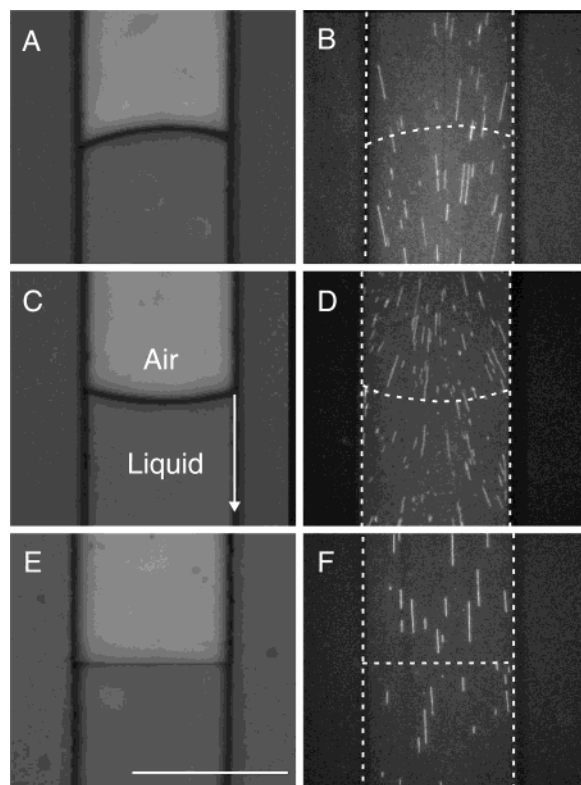


Figure 1. The shape of the air–water interface and the orientation of molecules of DNA that result from combing in a 100- μm Channel (A) Water spontaneously receded in the microchannel and produced a convex air–water interface. Speed: 0.5 $\mu\text{m/s}$. Effective dynamic contact angle is $\theta_m = 103^\circ$. (B) DNA stretched by the interface in A. (C) A concave interface was obtained when a vacuum was applied. Speed: 90 $\mu\text{m/s}$. Effective dynamic contact angle $\theta_m = 78^\circ$. (D) DNA stretched by the interface in B. (E) The rate of fluid withdrawal was adjusted to yield a flat air–water interface. Speed: 4 $\mu\text{m/s}$. Effective dynamic contact angle $\theta_m = 90^\circ$. (F) DNA stretched parallel to the walls of the channel by the interface in E. Scale bar represents 100 μm ; arrow indicates the direction of motion the air–water interface.

requires that the contact angle of the liquid to the solid, λ_{SL} , satisfy eq 2, where γ_{SV} is the interfacial tension between the solid and the vapor, γ_{SL} that between the solid and liquid, and γ_{LV} that between the liquid and the vapor.

$$\gamma_{\text{SV}} = \gamma_{\text{SL}} + \gamma_{\text{LV}} \cos \lambda_{\text{SL}} \quad (2)$$

In the absence of gravity, the force balance on a vapor–liquid interface reduces to the Young–Laplace equation (eq 3), where ΔP is the pressure drop across the vapor–liquid interface, and H is the mean curvature of the interface.

$$\Delta P = -2H \cdot \gamma_{\text{SL}} \quad (3)$$

The velocity of the resulting capillary linear flow is found by substituting the expression for the capillary pressure into Poiseuille’s equation.²⁷ This substitution gives eq 4, where l is the length of the plug, r the hydraulic radius, given by the ratio of the volume of fluid to the area of the solid–liquid interface, and η the viscosity of the fluid.

$$\frac{dl}{dt} = \frac{2 \cdot \gamma_{\text{LV}} \cdot r \cdot \cos \lambda}{8\eta} \quad (4)$$

In our experiments, we observed a decrease in this velocity as the water is replaced by air. These observations correspond to the inverse proportionality of the velocity to the length of the fluid plug in eq 4 and are therefore consistent with this model. The value of the effective contact angle measured as the interface was moving was 103° , nearly equal to the static contact angle of 100° . While the motion of the interface, in principle, leads to additional effects that alter its shape relative to the static case (see below), the contribution of these effects to the shape of the interface in Figure 1A appears secondary to that of the wetting properties of the wall under this particular set of conditions. In this case, the shape of the dynamic interface is similar to that of the static interface dictated by the Young–Laplace boundary conditions imposed at each wall.²⁸

The Rate of Fluid Withdrawal Affects the Shape of the Air–Water Interface. When pressure is applied to a plug of liquid inside the same 100- μm wide channel, the velocity of the air–water interface increases. This action decreases the effective dynamic contact angle of the liquid with the walls of the channel. This effect is illustrated in Figure 1C, which shows a concave air–water interface with an effective dynamic contact angle of $\theta_m = 78^\circ$ that resulted when the velocity of fluid flow was increased to 90 $\mu\text{m/s}$. All images in Figure 1 were obtained in a single channel, thereby ensuring constant channel height, width, and wall chemistry.

The shape of the air–water interface observed under these conditions is likely the result of a combination of three effects. The first contribution is the (convex) shape of the static interface, which is a function of the width of the channel and the static contact angle the interface makes with the walls of the channel.²⁸ The second contribution comes from the parabolic velocity profile known to develop within these channels, which has a curvature opposite that of the static interface. The third contribution is the friction between the air–water interface and the walls of the channel.

Though the way in which these factors combine to establish the dynamic interfacial shapes observed is not understood, we were able to vary the shape of the interface in a continuous fashion by altering the rate at which the fluid was withdrawn from the channel. In particular, we were able to obtain a flat interface, shown in Figure 1E, as an intermediate state between the convex interface (Figure 1A) that resulted from spontaneous flow and the concave interface (Figure 1C) that resulted from applying a larger pressure drop. The linear velocity of this interface was 4 $\mu\text{m/s}$.

In all three cases shown in Figure 1 the orientation of the chain axis of the DNA is perpendicular to the air–water interface. Accordingly, the concave interface resulted in DNA oriented in a half sunburst pattern, shown in Figure 1D, that is similar to that observed with the convex interface, shown in Figure 1B, except the pattern is reversed. Finally, Figure 1F illustrates that by adjusting the rate of withdrawal to obtain a flat interface, we were able to obtain molecules that were aligned parallel to the channel walls.

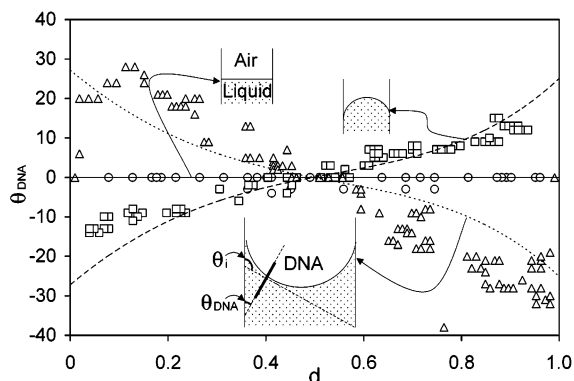


Figure 2. Relationship between the shape of the air–water interface and the orientation of stretched DNA. Data plotted as points correspond to the measured angles (θ_{DNA}) of individual DNA chains with respect to the walls of the channel along the normalized width of the channel (d), as depicted in the insert. Each case corresponds to one of the three cases shown in Figure 1: convex (\square , dashed line), concave (Δ , dotted line), and flat (\circ , solid line) air–water interface. Lines indicate chain angles predicted as the normal to the air–water interface across the width of the channel.

If the static contact angle alone dictated the shape of the air–water interface within microchannels, as in eq 3, a flat interface would be easily obtained by using a channel wall whose static contact angle with water is 90° . Since we achieved PDMS contact angles ranging from 17° to 100° by oxidation and subsequent exposure to air, we could simply oxidize the PDMS and let it relax until the contact angle reached 90° . As discussed here, the effective dynamic contact angle decreases relative to the static value with increasing velocity of the fluid. Consequently, the requirement for achieving a flat air–water interface, and thereby DNA molecules that are stretched with a parallel alignment of chains, is simply that the static contact angle between the wall of the channel and water be greater than 90° , a situation achieved with PDMS without further modification. A flat interface is then achieved by controlling the rate of flow of fluid out of the channel.

We quantify the effects of the geometry of the air–water interface on the orientation of the stretched molecules of DNA in Figure 2, which is a plot of the orientation of the DNA as a function of the distance from the wall in a $100\text{-}\mu\text{m}$ channel. The quantity plotted is the angle, θ_{DNA} , between the DNA and the left wall of the channel, as depicted in the inset; the orientation shown here was arbitrarily defined as a positive angle. Each set of data corresponds to one of the three cases in Figure 1: flat, concave, and convex interfaces. For each case, we also measured θ_{m} , the angle of the air–water interface responsible for orienting the DNA along the width of the channel; we then used these values to predict the orientation of the DNA by assuming that the DNA is stretched perpendicular to the interface.

For the case of the flat interface, the predicted angles – 90° along the entire width of the channel – are in close agreement with measured values. In the case of the convex interface, the agreement is only qualitative. The differences between measured and predicted values are likely due to the fact that we cannot pair interface shape and DNA orientation

precisely because our current setup does not allow their simultaneous imaging. These results do show a clear trend nonetheless. The concave case presents an additional effect near the edges of the channel. Though the shape of the air–water interface would dictate that the DNA molecules extend with positive angles on the left side of the channel and negative angles on the right, the channel walls prevent this extension and restrict the molecules to extending parallel to the walls. Omitting this effect, this case also shows good agreement between measured and predicted values. If shear flows within the microchannels were responsible for the orientation of the DNA, the chains would be aligned parallel to the fluid flow and thereby to the channel walls in all three cases shown in Figure 2. The variable orientation of the chains produced by the various interfacial shapes clearly shows that the molecules are being stretched and oriented by the local action of the air–water interface, which is consistent with the simple model of Bensimon et al. (eq 1).

The Width of the Channel Affects the Shape of the Air–Water Interface. In addition to the wetting properties and the rate of withdrawal of the solution, the width of the channel also affects the shape of the air–water interface. In the absence of externally applied pressure, the interface also receded spontaneously in $20\text{-}\mu\text{m}$ wide channels. In contrast to the $100\text{-}\mu\text{m}$ wide channels of the same height, the spontaneous capillary flow observed here yielded a nearly flat interface with no adjustments of the rate of flow, as shown in Figure 3A. We reason that in this case, the dynamic effects discussed previously just balance the static effects to produce this nearly flat interface. As expected, the DNA molecules combed with this configuration were aligned parallel to the walls of the channels, as shown in Figure 3B. When a pressure drop was applied, the results are equivalent to those obtained in the $100\text{-}\mu\text{m}$ channel. Figure 3C shows the concave interface, which stretched the molecules in the pattern shown in Figure 3D.

For $500\text{-}\mu\text{m}$ wide channels of the same height, a flat interface was not achievable. Instead, the shape of the air–water interface transformed from convex to concave through the undulated shape shown in Figure 4A, which led to more complicated patterns of DNA, as shown in Figure 4B. We rationalize this interface by reasoning that as the width increases, the effects of the wall chemistry lose importance in relation to the velocity of the fluid in the center of the channel. This effect underlines the challenge in describing how the various factors combine to determine the overall shape of the dynamic interface.

Directing the Path of the Interface Leads to Curved Molecules of DNA. While it is clear that molecular combing requires the adhesion of the ends of the DNA to the surface, we suspected the molecule also formed intermediate points of attachment. Figure 5A, which shows DNA bending around a corner as it is stretched, confirms this hypothesis. (The variations in contrast are due to the bundling of two or more molecules during stretching.) We speculate that as the DNA is stretched, its hydrophobic core is exposed periodically. The adhesion of these hydrophobic spots to the hydrophobic surface forms the mid-molecule anchor points. Judging from

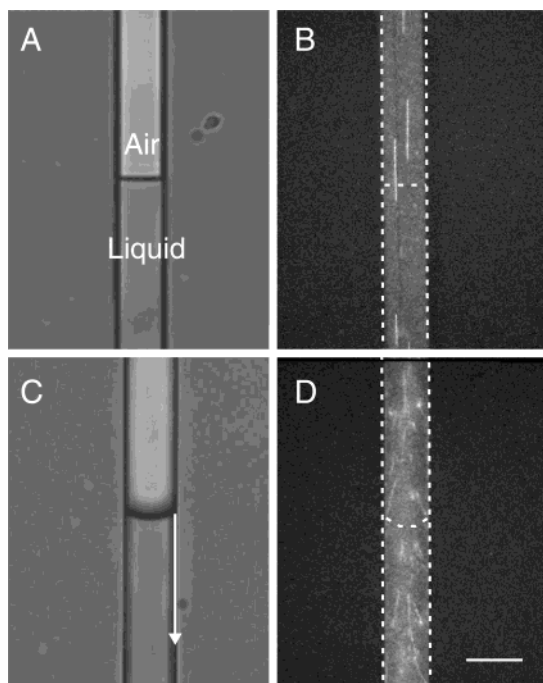


Figure 3. The shape of the air–water interface and the orientation of molecules of DNA that result from combing in a 20- μm channel. (A) Water spontaneously receded in the microchannel and produced a flat air–water interface. Speed: 5 $\mu\text{m}/\text{s}$. (B) DNA stretched parallel to channel walls by the flat interface in A. (C) A concave interface was obtained when vacuum was applied. Speed: 12 $\mu\text{m}/\text{s}$. (D) DNA stretched by the interface in (B). Scale bar represents 20 μm ; arrow indicates the direction of motion of the air–water interface.

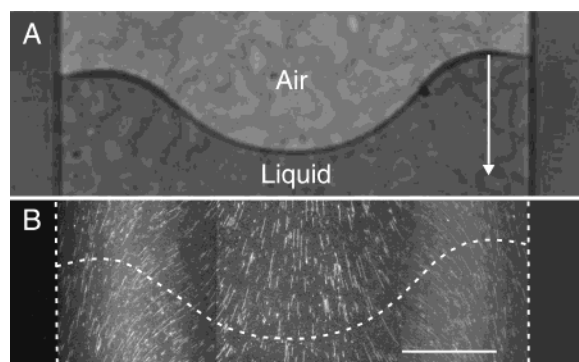


Figure 4. The shape of the air–water interface and the orientation of molecules of DNA that result from combing DNA in a 500- μm Channel. (A) The withdrawal of fluid through this microchannel produces an air–water interface with a complex shape. Speed: 900 $\mu\text{m}/\text{sec}$. (B) DNA stretched by the interface in A. Scale bar represents 100 μm ; arrow indicates the direction of motion of the air–water interface.

the continuous change in orientation observed for curved molecules, we estimate the DNA is attached to the substrate at anchor points that are spaced by less than one micron, the lower limit of what can be resolved optically and a distance that corresponds to approximately two thousand base pairs along the stretched chain. In addition, these observations indicate that the instantaneous shape of the air–water interface immediately in contact with the DNA dictates the direction of stretching at each point along a molecule.

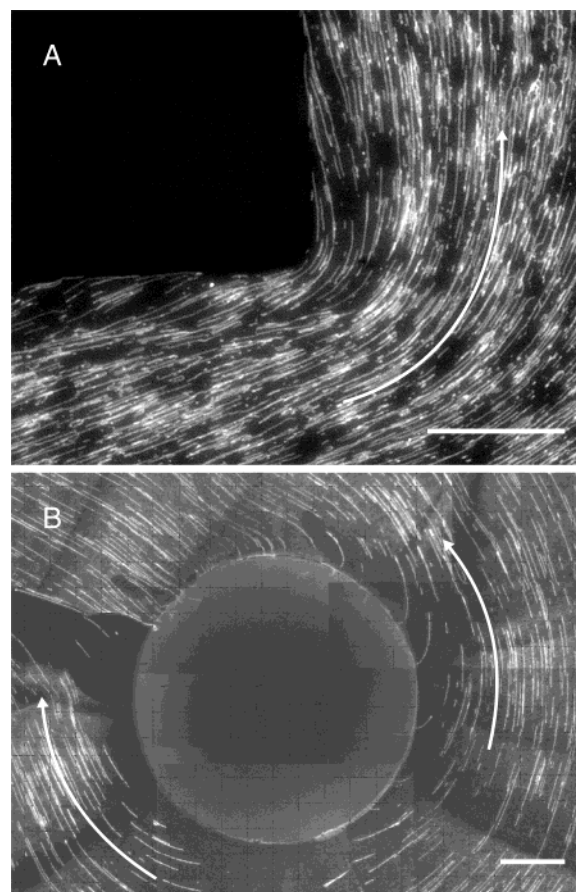


Figure 5. The air–water interface acts as a local field directing the orientation of molecules dynamically as they are deposited. Molecules of DNA oriented by passage of an air–water interface around (A) a 90° bend in a 100 μm channel, and (B) a 100- μm post. Scale bars in both cases represent 20 μm ; arrows indicate the direction of motion of the air–water interface.

We also deposited curved DNA chains by moving the air–water interface through an array of vertical cylindrical posts (Figure 5B). Because these posts had a diameter of 50 μm , the radius of curvature of the molecules deposited around the posts ranged from 50 μm for chains directly adjacent to the post to effectively infinity (i.e., straight), for chains sufficiently far ($> \sim 100 \mu\text{m}$) from the posts. In this way, the orientation of the molecules also acts as local reporter of the shape of the air–water interface as it proceeded around the post. These results indicate the opportunity for the controlled orientation of single molecules of DNA on surfaces.

Previously, Huang et al. used a technique similar to the one described in this work to direct the deposition of nanorods.²⁹ These objects were rigid and their orientation could not be varied along the length of the rod. Furthermore, functionalizing these nanorods with specific chemical groups is difficult. In contrast, the flexible backbone of the DNA molecule allows the orientation of the molecules to be altered as the chain is deposited. This ability to control orientation, in combination with the ease with which the chemical programmability can be manipulated, makes DNA an ideal candidate for bottom up assembly of nanosystems.

Conclusions. We have demonstrated the use of microchannels for creating micropatterned regions of stretched and oriented molecules of DNA. In contrast to traditional microarrays, in which each element contains a different short sequence, the arrays described in this paper consist of whole molecules of a single type of DNA that are stretched on the surface. This approach allowed us to precisely control both the location and the orientation of the elongated molecules through adjustments to the shape of the receding contact line. We have shown that although the way in which several factors (the wall chemistry of the channel, the speed of fluid withdrawal, and the geometry of the cross section of the channel) combine in dictating this shape is complex, we were able to adjust them to obtain the desired interfacial geometry. We have also shown that it is the local, instantaneous shape of this interface that dictates the orientation of the deposited DNA, namely, that the DNA is always stretched perpendicular to the interface, even when the orientation of the interface changes as the chain is stretched and deposited. These observations are consistent with the theory by Bensimon et al., which postulates that the molecules are stretched by the surface tension of the air–liquid interface.

The COMMIC technique itself is limited only by the resolution of photolithography, which is about one micron. However, since the DNA used here stretches to a length of about 20 microns, the limiting size of useful arrays is about 50 microns. We have also shown that with the appropriate choice of channel features we were able to orient DNA chains with different radii of curvature. Parallel arrays of chains were also produced using a flat air–water interface. Such patterns will be useful in developing arrays for automating molecular combing for high-throughput applications in genetic analysis.

We believe the ability to micropattern parallel DNA molecules will be valuable not only for genomics, but also as templates for the fabrication of arrays of metallic and semiconducting nanowires. This paper illustrates the level of control over the location, orientation, and curvature of DNA templates that may be achieved by using microfluidic flow.

Acknowledgment. This work was supported in part by the NASA University Research, Engineering and Technology Institute on Bio Inspired Materials (BIMat) under award No. NCC-1-02037 and the National Science Foundation Materials Research Science and Engineering Center at Princeton under award no. DMR-9809483. C.A.P.P. thanks the National Science Foundation for support through a Graduate Research Fellowship.

Supporting Information Available: Detailed experimental procedures. This material is available free of charge via the Internet at <http://pubs.acs.org>.

References

- (1) Whitesides, G. M.; Mathias, J. P.; Seto, C. T. *Science* **1991**, *254*, 1312–1319.
- (2) Hecht, S. *Angew. Chem., Int. Ed.* **2003**, *42*, 24–26.
- (3) Mirkin, C. A. *Inorg. Chem.* **2000**, *39*, 2258–2272.
- (4) Niemeyer, C. M. *Angew. Chem., Int. Ed.* **2001**, *40*, 4128–4158.
- (5) Seeman, N. C. *Nature* **2003**, *421*, 427–431.
- (6) Harnack, O.; Ford, W. E.; Yasuda, A.; Wessels, J. M. *Nano Lett.* **2002**, *2*, 919–923.
- (7) Monson, C. F.; Woolley, A. T.; *Nano Lett.* **2003**, *3*, 359–363.
- (8) Keren, K.; Krueger, M.; Gilad, R.; Ben-Yoseph, G.; Sivan, U.; Braun, E. *Science* **2002**, *297*, 72–75.
- (9) Bensimon, A.; Simon, A.; Chiffaudel, A.; Croquette, V.; Heslot, F.; Bensimon, D. *Science* **1994**, *265*, 2096–2098.
- (10) Bensimon, D.; Simon, A. J.; Croquette, V.; Bensimon, A. *Phys. Rev. Lett.* **1995**, *74*, 4754–4757.
- (11) Allemand, J.-F.; Bensimon, D.; Jullien, L.; Bensimon, A.; Croquette, V. *Biophys. J.* **1997**, *73*, 2064–2070.
- (12) Michalet, X.; Ekong, R.; Fourgerousse, F.; Rousseaux, S.; Schurra, C.; Hornigold, N.; van Slegtenhorst, M.; Wolfe, J.; Povey, S.; Beckmann, J. S.; Bensimon, A. *Science* **1997**, *277*, 1518–1523.
- (13) Herrick, J.; Michalet, X.; Conti, C.; Schurra, C.; Bensimon, A. *Proc. Natl. Acad. Sci. U.S.A.* **2000**, *97*, 222–227.
- (14) Gueroui, Z.; Place, C.; Freyssingheas, E.; Berge, B. *Proc. Natl. Acad. Sci. U.S.A.* **2002**, *99*, 6005–6010.
- (15) Richter, J.; Seidel, R.; Kirsh, R.; Mertig, M.; Pompe, W.; Plaschke, J.; Schackert, H. K. *Adv. Mater.* **2000**, *12*, 507–510.
- (16) Yokota, H.; Sunwoo, J.; Sarikaya, M.; van den Engh, G.; Aebersold, R. *Anal. Chem.* **1999**, *71*, 4418–4422.
- (17) Zimmermann, R. M.; Cox, E. C. *Nucleic Acids Res.* **1994**, *22*, 492–497.
- (18) Namasivayam, V.; Larson, R. G.; Burke, D. T.; Burns, M. A. *Anal. Chem.* **2002**, *74*, 3378–3385.
- (19) Klein, D. C. G.; Gurevich, L.; Janssen, J. W.; Kouwenhoven, L. P.; Carbeck, J. D.; Sohn, L. L. *Applied Phys. Lett.* **2001**, *78*, 2396–2398.
- (20) Woolley, A. T.; Kelly, R. T.; *Nano Lett.* **2001**, *1*, 345–348.
- (21) Yokota, H.; Johnson, F.; Lu, H.; Robinson, R. M.; Belu, A. M.; Garrison, M. D.; Ratner, B. D.; Trask, B. J.; Miller, D. L. *Nucleic Acids Res.* **1997**, *25*, 1064–1070.
- (22) Ohtobe, K.; Ohtani, T. *Nucleic Acids Res.* **2001**, *29*, e109–114.
- (23) Jing, J.; Reed, J.; Huang, J.; Hu, X.; Clarke, V.; Edington, J.; Housman, D.; Anantharaman, T. S.; Huff, E. J.; Misha, B.; Porter, B.; Shenker, A.; Wolfson, E.; Hiort, C.; Kantor, R.; Aston, C.; Schwartz, D. C. *Proc. Natl. Acad. Sci. U.S.A.* **1998**, *95*, 8046–8051.
- (24) Channels were fabricated using soft lithography, as described in ref 25. The top and walls were cast out of PDMS, while the bottom consisted of a polystyrene-coated glass slide.
- (25) Xia, Y.; Whitesides, G. M. *Angew. Chem., Int. Ed.* **1998**, *37*, 550–575.
- (26) Miller C. A.; Neogi, P. *Interfacial Phenomena: Equilibrium and Dynamic Effects*, Dekker: New York, 1985; Vol. 17, pp 54–58.
- (27) Myer, D. *Surfaces, Interfaces, and Colloids: Principles and Applications*, VCH Publishers: New York, 1991; pp 103–104.
- (28) Davis, H. T. *Statistical Mechanics of Phases, Interfaces, and Thin Films*, VCH Publishers: New York, 1996; pp 333–352.
- (29) Huang, Y.; Duan, X.; Wei, Q.; Lieber, C. M. *Science* **2001**, *291*, 630–633.

NL034341X